

5-3-2019


Yeast mitochondrial protein Pet111p binds directly to two distinct targets in COX2 mRNA, suggesting a mechanism of translational activation

Julia L Jones
Rowan University

Katharina B. Hofmann
Max Planck Institute for Biophysical Chemistry

Andrew T. Cowan
Rowan University

Dmitry Temiakov
Follow this and additional works at: <https://jdc.jefferson.edu/bmpfp>
Thomas Jefferson University

 Part of the [Medical Molecular Biology Commons](#)

Patrick Cramer
Max Planck Institute for Biophysical Chemistry

[Let us know how access to this document benefits you](#)

Recommended Citation

See next page for additional authors

Jones, Julia L; Hofmann, Katharina B.; Cowan, Andrew T.; Temiakov, Dmitry; Cramer, Patrick; and Anikin, Michael, "Yeast mitochondrial protein Pet111p binds directly to two distinct targets in COX2 mRNA, suggesting a mechanism of translational activation" (2019). *Department of Biochemistry and Molecular Biology Faculty Papers*. Paper 153.

<https://jdc.jefferson.edu/bmpfp/153>

This Article is brought to you for free and open access by the Jefferson Digital Commons. The Jefferson Digital Commons is a service of Thomas Jefferson University's [Center for Teaching and Learning \(CTL\)](#). The Commons is a showcase for Jefferson books and journals, peer-reviewed scholarly publications, unique historical collections from the University archives, and teaching tools. The Jefferson Digital Commons allows researchers and interested readers anywhere in the world to learn about and keep up to date with Jefferson scholarship. This article has been accepted for inclusion in Department of Biochemistry and Molecular Biology Faculty Papers by an authorized administrator of the Jefferson Digital Commons. For more information, please contact: JeffersonDigitalCommons@jefferson.edu.

Authors

Julia L. Jones, Katharina B. Hofmann, Andrew T. Cowan, Dmitry Temiakov, Patrick Cramer, and Michael Anikin



Yeast mitochondrial protein Pet11p binds directly to two distinct targets in COX2 mRNA, suggesting a mechanism of translational activation

Received for publication, August 14, 2018, and in revised form, March 10, 2019. Published, Papers in Press, March 25, 2019, DOI 10.1074/jbc.RA118.005355

Julia L. Jones^{‡§}, Katharina B. Hofmann[¶], Andrew T. Cowan^{§1}, Dmitry Temiakov^{||}, Patrick Cramer[¶], and Michael Anikin^{§2}

From the [‡]Graduate Program in Cell and Molecular Biology, Graduate School of Biomedical Sciences and the [§]Department of Cell Biology & Neuroscience, Rowan University School of Osteopathic Medicine, Stratford, New Jersey 08084, the [¶]Department of Molecular Biology, Max Planck Institute for Biophysical Chemistry, 37077 Göttingen, Germany, and the ^{||}Department of Biochemistry & Molecular Biology, Sidney Kimmel Cancer Center, Thomas Jefferson University, Philadelphia, Pennsylvania 19107

Edited by Karin Musier-Forsyth

The genes in mitochondrial DNA code for essential subunits of the respiratory chain complexes. In yeast, expression of mitochondrial genes is controlled by a group of gene-specific translational activators encoded in the nucleus. These factors appear to be part of a regulatory system that enables concerted expression of the necessary genes from both nuclear and mitochondrial genomes to produce functional respiratory complexes. Many of the translational activators are believed to act on the 5'-untranslated regions of target mRNAs, but the molecular mechanisms involved in this regulation remain obscure. In this study, we used a combination of *in vivo* and *in vitro* analyses to characterize the interactions of one of these translational activators, the pentatricopeptide repeat protein Pet11p, with its presumed target, COX2 mRNA, which encodes subunit II of cytochrome *c* oxidase. Using photoactivatable ribonucleoside-enhanced cross-linking and immunoprecipitation analysis, we found that Pet11p binds directly and specifically to a 5'-end proximal region of the COX2 transcript. Further, we applied *in vitro* RNase footprinting and mapped two binding targets of the protein, of which one is located in the 5'-untranslated leader and the other is within the coding sequence. Combined with the available genetic data, these results suggest a plausible mechanism of translational activation, in which binding of Pet11p may prevent inhibitory secondary structures from forming in the translation initiation region, thus rendering the mRNA available for interaction with the ribosome.

The yeast cytochrome *c* oxidase (COX)³ complex is an assembly of 12 subunits (1), of which only three, Cox1p, Cox2p, and Cox3p, are encoded by mitochondrial DNA, whereas the others are the products of nuclear genes. A regulatory system must therefore be in place to ensure coordinated expression from both genomes, such that all of the subunits are produced synchronously and stoichiometrically for the correct assembly of the complex (2). This system appears to utilize a set of nuclear DNA-encoded messengers that act in a gene-selective manner to authorize the mitochondrial mRNAs to undergo translation (2–4). Expression of subunit II of COX, Cox2p, is under the control of one of such messengers, the product of the nuclear gene *pet111* (5, 6). Genetic characterization has demonstrated that the product of this gene, Pet11p, sanctions the translation of COX2 by acting in the 5'-UTR of the mRNA (7) and thereby limits the production of Cox2p under physiologic conditions (8). As is the case with most yeast mitochondrial gene-specific translational activators (3), Pet11p is anchored to the matrix surface of the inner mitochondrial membrane, thus enabling co-translational insertion of the nascent Cox2p into the membrane (8). This function of Pet11p appears to be of critical importance because Cox2p failed to accumulate when translated away from the membrane (9). At the membrane, Pet11p is associated in a complex, which also includes translational activators specific to COX1, COX3, and COB (10, 11). This suggests an additional function of the translational activators to ensure proper spatial coordination during the production and assembly of respiratory complexes III and IV. All of these interactions presumably take place in the framework of the recently discovered MIOREX super complex, which is responsible for the organization of mitochondrial gene expression (12).

The finding that Pet11p functionally interacts with the 5'-UTR of COX2 (7, 13) to enable translation invited a suggestion that the protein may bind to the mRNA directly. However,

This work was supported by New Jersey Health Foundation Grant PC127-13 (to M. A.) and by the Rowan University Graduate School of Biomedical Sciences (to J. L. J.). The authors declare that they have no conflicts of interest with the contents of this article.

This article contains supporting text, Table S1, and Figs. S1 and S2.

The data discussed in this publication have been deposited in NCBI's Gene Expression Omnibus and are accessible through GEO Series accession number GSE117899.

¹ Present address: Dept. of Pharmacy, Thomas Jefferson University Hospital, 111 South 11th St., Suite 2260, Philadelphia, PA 19107.

² To whom correspondence should be addressed: Dept. of Cell Biology & Neuroscience, Rowan University School of Osteopathic Medicine, 42 East Laurel Rd., UDP 2200, Stratford, NJ 08084. Tel.: 856-566-6326; Fax: 856-566-2881; E-mail: anikinmi@rowan.edu.

³ The abbreviations used are: COX, cytochrome *c* oxidase; EMSA, electrophoretic mobility shift assay; MPP, mitochondrial processing peptidase; nt, nucleotide; PAR-CLIP, photoactivatable ribonucleoside-enhanced cross-linking and immunoprecipitation; PPR, pentatricopeptide repeat; PMF, peptide mass fingerprinting; TAP, tandem affinity purification; NSC, non-specific control; Ni-IDA, iminodiacetic acid.

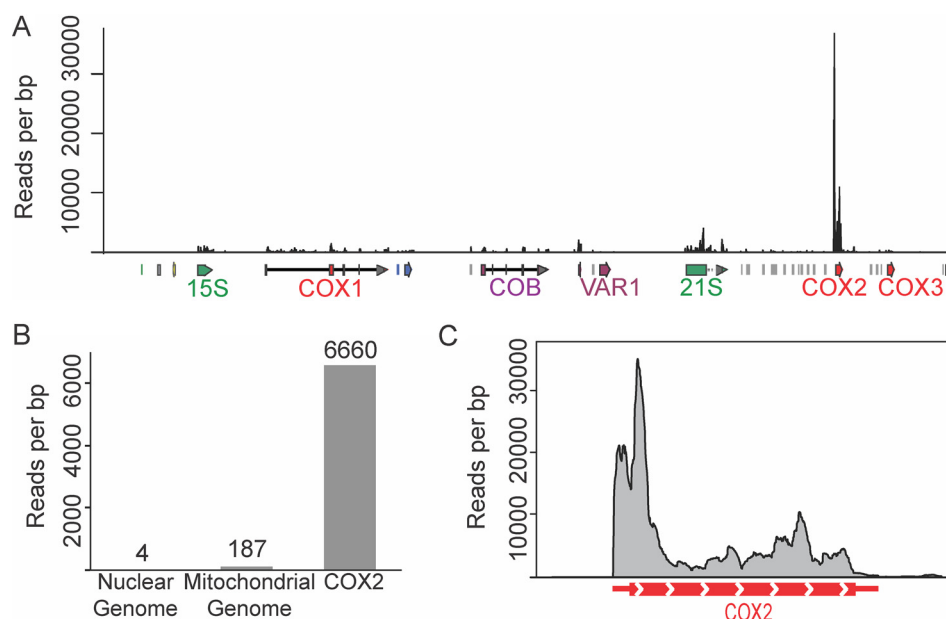


Figure 1. Pet111p is predominantly associated with COX2 mRNA *in vivo*. A, PAR-CLIP analysis of cells expressing Pet111p-TAP was performed, and the resulting RNA reads were aligned to the yeast mitochondrial genomic sequence. B, the abundance of the RNA reads associated with the nuclear and mitochondrial genomic sequences was compared with that of the *cox2*-associated reads. C, a portion of the alignment in A showing the distribution of the sequencing reads in the vicinity of the *cox2* gene. The position of the coding sequence is indicated by the red bar with the arrows showing the direction of translation. The red lines correspond to the untranslated regions of the mature mRNA.

a direct binding of Pet111p to COX2, or any other RNA, has not yet been demonstrated. In this study, we evaluated Pet111p for its potential to interact with RNA both *in vivo* and *in vitro*. Using photoactivatable ribonucleoside-enhanced cross-linking and immunoprecipitation (PAR-CLIP) analysis, we confirmed that Pet111p preferentially associates with the 5'-end proximal portion of COX2 mRNA. Further analysis by a combination of electrophoretic mobility shift assay (EMSA) and RNase footprinting revealed two distinct binding targets of the protein, one close to the 5'-end of the transcript and one in the beginning of the coding sequence. Based on the positions of the binding targets and taking into account the results of genetic analysis and the prediction of the structural organization of the RNA, we suggest plausible mechanisms by which binding of Pet111p could facilitate translation of COX2.

Results

Pet111p directly contacts COX2 mRNA *in vivo*

To examine whether Pet111p is engaged in direct contacts with RNA *in vivo*, we carried out an unbiased analysis using PAR-CLIP. Yeast expressing tandem affinity purification (TAP)-tagged Pet111p (Pet111p-TAP) were grown in the presence of 4-thiouracil and UV-irradiated to induce the formation of RNA-protein cross-linking products. The cells were then lysed, and the lysate was subjected to immunoprecipitation using anti-TAP-tag antibodies. The co-precipitated RNA species were trimmed with RNase T1, and the presence of Pet111p-TAP in the resulting immunoprecipitate was confirmed by Western blotting (Fig. S1). The photocross-linked RNA in a part of the sample was 5'-³²P-labeled and analyzed by SDS-PAGE. As shown in Fig. S1, a population of radioactive species with an electrophoretic mobility approximately corresponding to Pet111p-TAP was dominant on the gel. We inter-

preted these species as RNA-Pet111p-TAP cross-linking products. After adapter ligation, the cross-linked RNA was converted into cDNA and PCR-amplified, and the amplification products were subjected to deep sequencing. The collected sequencing reads 20–50 nucleotides (nt) in length aligned with the sequence of mitochondrial DNA are presented in Fig. 1A. The alignment showed that the vast majority of the reads belonged to COX2 mRNA. Although some background levels of the RNA in the sample originated from the nuclear genome or represented other mitochondrial genes, the RNA sequences associated with COX2 were over 30 times more abundant (Fig. 1B). Within the COX2 mRNA (Fig. 1C), the density of the reads was significantly higher in the 5'-end proximal region, including the 5'-UTR and ~60 nucleotides into the beginning of the coding sequence. These results confirm that Pet111p is indeed an RNA-binding protein that selectively interacts with COX2 *in vivo* with a particularly high affinity to the 5'-end region of the mRNA.

Expression of recombinant Pet111p

To determine whether Pet111p requires additional mitochondrial factors to bind to COX2 and to define its binding target (or targets) with greater precision, we purified a recombinant form of the protein and used it to assemble and evaluate complexes with synthetic RNA oligonucleotides of defined length and sequence. As is the case for most nucleus-encoded mitochondrial proteins, Pet111p is expected to undergo N-terminal processing during import into mitochondria. We intended to generate a recombinant form of the mature protein; however, to the best of our knowledge, the processing site of Pet111p has never been experimentally established. To determine the site of maturation, we took advantage of an available library of yeast ORFs inserted into the BG1805 expression vec-

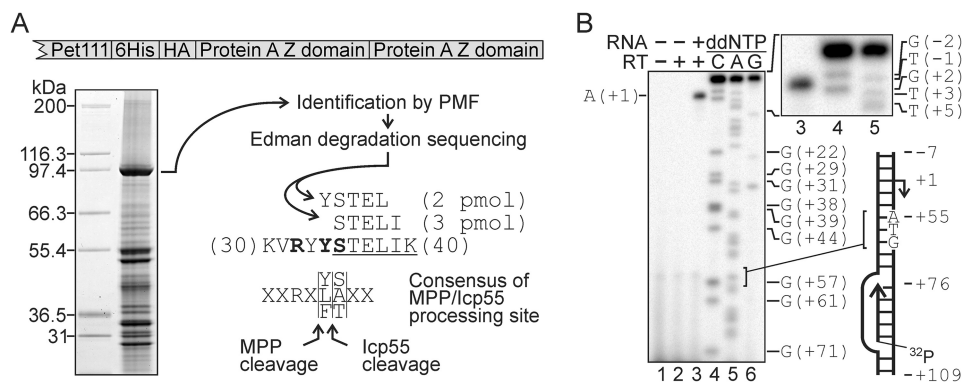


Figure 2. Characterization of the processing of Pet11p and COX2 in mitochondria. A, an image of a Coomassie-stained polyacrylamide gel showing the proteins in a preparation of tagged Pet11p partially purified from yeast mitochondria. The composition of the C-terminal purification tag is shown above the image. The positions of the hexahistidine (6His) and hemagglutinin epitope (HA) tags are indicated. The protein in the indicated band was identified as Pet11p by PMF, and Edman degradation analysis of the protein revealed two sequence reads, pointed to by the bent arrows. The reads are aligned with a portion of the Pet11p sequence (numbers indicate positions of the flanking amino acid in the sequence of the Pet11p precursor), in which the determined N-terminal sequence of the mature protein is underlined. The amino acids represented by bold letters match the consensus of the MPP/Icp55 processing site (37), which is shown below the alignment. The sites of cleavage by MPP and Icp55 are indicated by arrows. B, a phosphorimaging scan of an area of a polyacrylamide gel showing the products of extension of a 5'-³²P-labeled DNA primer COX2-96–76. The primer was hybridized to COX2 mRNA in a total mitochondrial RNA isolate and extended with RT (lane 3). Control lanes 1 and 2 contained, respectively, the unextended primer and the primer extended in the absence of mitochondrial RNA. The length of the product of extension in lane 3 was determined by a comparison with DNA size markers (lanes 4–6). The markers were generated by extension of the primer in the presence of 2',3'-dideoxynucleoside triphosphates as specified above the image. The dsDNA template used in the primer extension reactions contained a sequence of the *cox2* promoter between positions –7 and +109 relative to the start site (+1), as explained by the scheme to the right. The bands in lane 4 are assigned on the right of the image, and the position on the gel that corresponds to the initiation codon is indicated by brackets. An area on the top of the image is enlarged to show the slow-running bands in lanes 3–5 more clearly, and the bands in lanes 4 and 5 are assigned on the right. Comparison with the size markers indicates that the 3'-end of the product of primer extension in lane 3 corresponds to position +1.

tor (14) that provides a C-terminally fused hexahistidine tag. We overexpressed the tagged Pet11p in yeast, isolated the mitochondrial fraction, and partially purified the processed form of the protein using Ni-IDA beads under denaturing conditions. Analysis of the preparation by PAGE (Fig. 2A) revealed a major band running at ~97 kDa, and the protein in the band was further identified as Pet11p by peptide mass fingerprinting (PMF) (15). Edman degradation analysis of the protein returned two overlapping sequences: STELI and YSTEL. We therefore concluded that Pet11p undergoes a two-step processing with mitochondrial processing peptidase (MPP) cleaving a 33-amino acid peptide at Tyr-33 and Icp55p removing residue Tyr-34 (Fig. 2A). Based on these data, we constructed a plasmid for bacterial expression of a mature form of Pet11p, in which an N-terminal histidine purification tag (MAH₆) was fused to amino acid Ser-35 of the protein. This recombinant form of the protein is referred to as rPet11p in this study. Expression in *Escherichia coli* at a reduced temperature and low induction levels allowed us to obtain rPet11p in a soluble form. The protein was purified to homogeneity by a preliminary enrichment with Ni-IDA beads followed by heparin affinity chromatography and gel filtration (Fig. S2A). Surprisingly, the apparent electrophoretic mobility of rPet11p corresponded to a molecular mass of ~70 kDa, which was substantially lower than the calculated value of 91.3 kDa. To exclude the possibility that this shift was due to a truncation that might have occurred during the expression, we determined the actual molecular mass of the protein in the preparation by MALDI-TOF-MS. As shown in Fig. S2B, the observed molecular mass of rPet11p was in agreement with the expected value.

COX2 mRNA does not undergo maturation at the 5'-end

Several yeast mitochondrial mRNAs have been shown to undergo Pet127p-dependent trimming at the 5'-end following

endonucleolytic processing of the primary transcripts (16). The position of the 5'-end in mature COX2 was previously mapped to coincide with the start site of the *cox2* promoter (17). The mapping was performed at a single-nucleotide resolution by extension of a DNA primer hybridized to COX2 with RT. However, the 3'-end of the primer used in the study corresponded to position 33 inside the 5'-UTR; thus, had the trimming shifted the 5'-end into the region between that point and the translational start site, the experiment would fail to detect the maturation product. Therefore, to design the RNA oligonucleotides for the *in vitro* reconstruction of the rPet11p–RNA complexes, we needed to verify the position of the 5'-end in mature COX2. We repeated the primer extension experiment shifting the entire primer to a location inside the coding sequence. As shown in Fig. 2B, extension of the primer did not terminate near the area of the initiation codon and produced a larger single product. Comparison with a set of DNA size markers placed the 3'-end of the product to the position corresponding to +1 of the primary transcript, consistent with published data (17). This allowed us to conclude that COX2 does not undergo a 5'-end trimming, and thus the entire sequence of its 5'-UTR was included in the evaluation of interaction with rPet11p.

rPet11p specifically binds *in vitro* to at least two distinct targets in the 5'-end proximal region of COX2

Our PAR-CLIP analysis showed that Pet11p interacts with RNA directly and specifically *in vivo*. To examine whether the protein retains this ability in the absence of other mitochondrial factors, we used EMSA. In this experiment, radioactively labeled RNA probes of defined sequence were incubated with rPet11p to allow the formation of complexes, which were then separated from free RNA by native PAGE. We first compared two RNA probes, of which one encompassed the entire COX2 5'-UTR (COX2–1–54), and the other represented a sequence

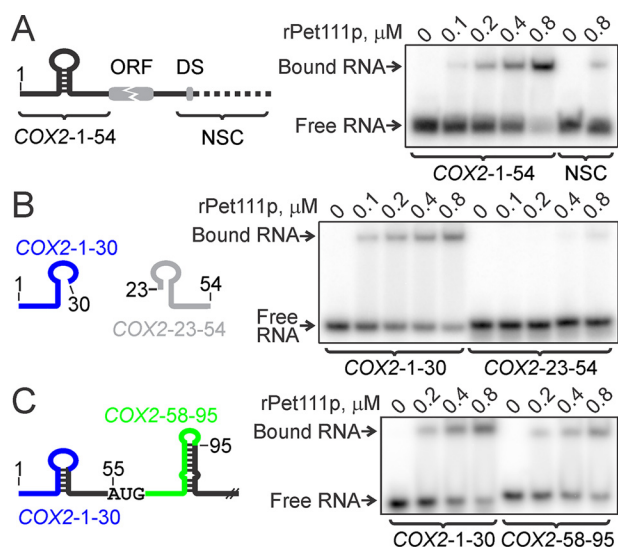


Figure 3. rPet11p binds to specific regions of COX2 mRNA *in vitro*. The labeled RNA probes shown in the schemes to the left were incubated with varying concentrations of rPet11p and resolved by native PAGE. A, the binding efficiency of two probes was compared, one spanning the entire 5'-UTR and the other corresponding to a sequence downstream of the ORF (NSC). DS marks the position of a conserved dodecameric sequence (38), and the dashed line indicates the region not present in the mature COX2 (17). B, two overlapping probes were designed to cover the sequence of the 5'-UTR, and their interaction with rPet11p was compared. C, the binding efficiency of the COX2-1-30 probe was compared with that of a probe (COX2-58-95) representing a sequence in the beginning of the ORF.

downstream from the coding sequence (nonspecific control (NSC)). As shown in Fig. 3A, EMSA revealed prominent bands corresponding to the COX2-1-54-rPet11p complex, whereas NSC failed to complex appreciably with the protein. We conclude that rPet11p can discriminate between RNA molecules independently of other mitochondrial proteins and that the 5'-UTR harbors a binding target of the protein.

A relatively stable stem-loop structure has been predicted to form upstream of the ORF of COX2 (18). It resides within a 31-nt region, which has been shown to contain residues required for respiration (19), suggesting that the stem-loop might be a target of Pet11p. To evaluate this possibility, we used an overlapping pair of RNA probes, which covered the entire sequence of the 5'-UTR, but were positioned in such a way that the stem-loop structure could not form in either probe. If this structure was required for binding to Pet11p, we would expect to see a loss of the complex formation with both probes. However, as shown in Fig. 3B, whereas the COX2-23-54 probe failed to form a complex, the 5'-end proximal probe (COX2-1-30) retained the ability to interact with the protein. These results indicate that a binding target of Pet11p resides within the sequence of COX2-1-30 and argue against the involvement of the stem-loop as a major binding or specificity determinant. Considering that no secondary structure is expected to form within COX2-1-30, Pet11p can thus be classified as a sequence-specific single-stranded RNA-binding protein.

The high abundance of the PAR-CLIP sequencing reads at the site of translation initiation of COX2 (Fig. 1C) prompted us to examine whether that region had an additional binding target for Pet11p. The probe used in this experiment (COX2-

58-95) extended from just downstream of the initiation codon to the descending strand of a predicted stem-loop structure (20) located in the beginning of the coding sequence. EMSA revealed that this probe could readily complex with rPet11p with an affinity comparable with that of the COX2-1-30 probe, which was used as a positive control (Fig. 3C). Therefore we conclude that at least two Pet11p-binding targets are present in the 5'-end proximal region of COX2: one in the beginning of the 5'-UTR and one downstream from the initiation codon, and that the protein can recognize both targets independently of other mitochondrial factors.

The two mapped RNA targets of Pet11p share little similarity

Our EMSA results indicated the presence of Pet11p-binding targets in the RNA probes COX2-1-30 and COX2-58-95. To define the targets with greater precision, we employed RNase I footprinting (21). 5'-³²P-labeled COX2-1-30 was subjected to limited digestion with RNase I, and the products of digestion were separated at a single-nucleotide resolution (Fig. 4A, lane 2). RNase I is known to cleave poorly at GMP residues (22), and thus the weak band corresponding to the product of cleavage at G22 was readily identifiable and provided a reference point to assign other bands in the lane. The pattern of the cleavage products was reasonably uniform throughout the probe, except at the purine-rich 3'-end where the cleavage was somewhat less prominent, suggesting that the probe was free of secondary structures. The probe was also incubated with rPet11p to allow the formation of a complex, the complex was treated with RNase I, and the products of digestion were separated (Fig. 4A, lane 3). The pattern of the cleavage was clearly different in the presence of rPet11p. As evident from the traces representing the distribution of radioactivity in lanes 2 and 3, the cleavage efficiency decreased drastically in a region close to the middle of the probe while increasing toward the ends. For each RNA fragment 2-29 nt in length, the effect of rPet11p was plotted as a logarithm of the intensity ratio in lanes 2 and 3 (bar plot in Fig. 4A). The positive-value bars in the plot indicated the residues in the RNA, at which RNase I cleavage was partially blocked by rPet11p. The most prominent protection was observed between positions 7 and 19, suggesting the presence of a Pet11p-binding target within these boundaries. In a similar way, probe COX2-58-95 was subjected to RNase I in the absence or presence of rPet11p (Fig. 4B). The cleavage products were quantified and analyzed as described above, and a region between positions 66 and 85 was identified as partially protected by the protein, which defined the boundaries of a second binding target of rPet11p. The clear footprints observed with both RNA probes attested once again to the ability of rPet11p to discriminate in favor of certain sequences in a single-stranded RNA context. As shown in Fig. 4C, the positions of the two mapped targets correlated with the areas in the COX2 mRNA where the PAR-CLIP sequence reads were the most abundant. Interestingly, the peaks of the density of the reads were somewhat shifted downstream relative to the rPet11p-binding targets, probably reflecting a bias imposed by the PAR-CLIP method.

The finding that the two mapped targets of rPet11p substantially differ in length (13 nt versus 21 nt in the 5'-UTR and

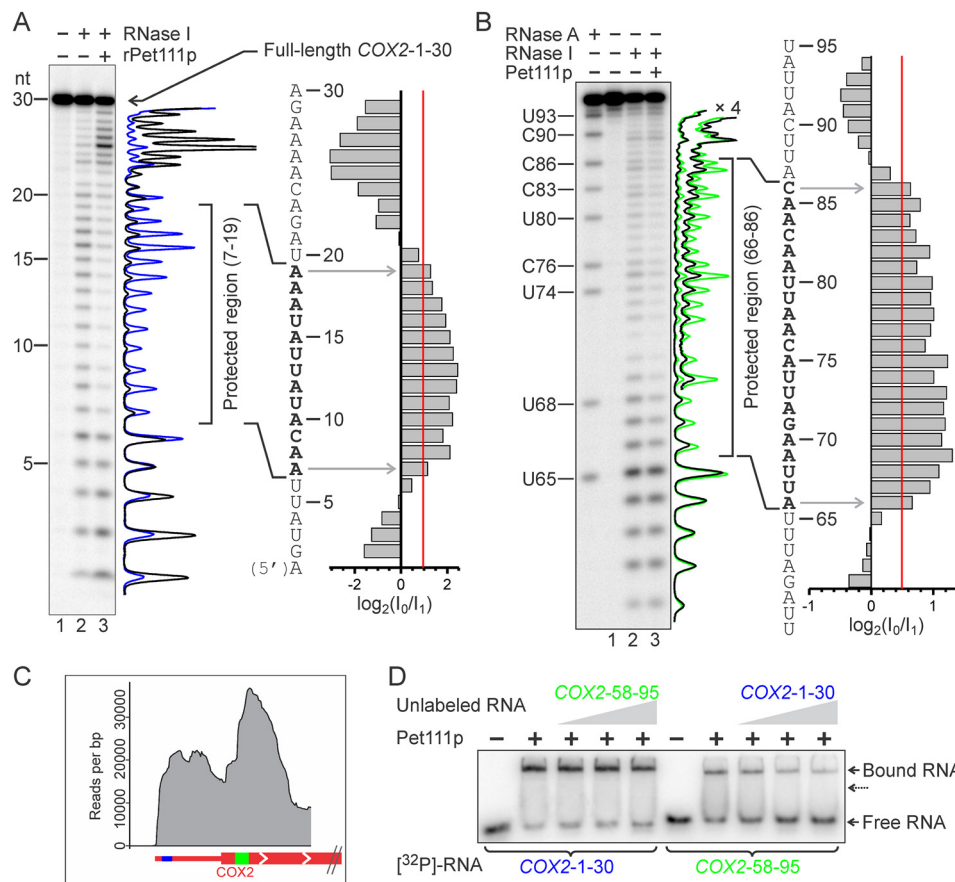


Figure 4. rPet111p recognizes two distinct targets in the 5'-end proximal region of COX2 mRNA. A, 5'-³²P-labeled COX2-1-30 RNA (0.6 μM) was digested with RNase I in the absence or presence of rPet111p (0.8 μM). The cleavage products were resolved by denaturing PAGE. The traces represent the distribution of radioactivity within lanes 2 (blue) and 3 (black). For each RNA fragment 2–29 nt in length, intensities of the corresponding bands in lanes 2 (I₀) and 3 (I₁) are plotted as log₂(I₀/I₁). Positions in the RNA, at which the bars in the plot exceeded 55% of the average of all positive-value bars (red line) were considered protected by rPet111p and are indicated by bold letters in the sequence of COX2-1-30. B, 5'-³²P-labeled COX2-58-95 (0.3 μM) was treated with RNase I in the absence or presence of rPet111p (0.6 μM), and the digestion products were resolved by PAGE. Digestion with RNase A was performed to generate RNA size markers (left lane). The traces and the bar plot on the right are as in A. The green and black traces correspond to lanes 2 and 3, respectively. C, a region of the alignment of the PAR-CLIP reads (Fig. 1) is shown. The positions of the two identified targets of rPet111p are indicated in blue (5'-UTR) and green (ORF). D, 5'-³²P-labeled COX2-1-30 was incubated with 0.8 μM rPet111p. The formed complex was resolved from the unbound probe in a native gel. Where indicated, unlabeled COX2-58-95 was present in the mixtures (0.2, 0.4, and 0.8 μM). In a reciprocal experiment (right side of the image), the labeled probe was COX2-58-95, and the unlabeled competitor was COX2-1-30. The dotted arrow points to the expected position of rPet111p bound to both RNA probes.

ORF targets, respectively) and share little sequence similarity was surprising. To account for this observation, one can assume that Pet111p might harbor two RNA-binding sites, of which each recognizes one of the two targets. Hypothetically, the protein could then associate with both targets simultaneously if the two binding sites worked independently. To test whether this was the case, we used EMSA to resolve the complexes that were formed by rPet111p in the presence of both COX2-1-30 and COX2-58-95 (Fig. 4D). In the first set of samples, the radiolabeled probe COX2-1-30 was present at a fixed concentration, whereas the concentration of COX2-58-95, which was not labeled, was gradually increased. Because of the basic nature of the protein, the electrophoretic mobility of the complexes is mostly controlled by their charge. Thus, within the range of the lengths of the RNA probes used in the study, the longer the RNA associated with rPet111p, the greater the mobility of the complex. Accordingly, if the COX2-58-95 probe were to bind to the radiolabeled COX2-1-30-rPet111p binary complex, the radioactive band of this ternary complex would be expected to appear between the bands corresponding to the

free RNA and the binary complex. However, we did not observe a band of the ternary complex either with this set of samples or in a reciprocal experiment where the radioactive probe COX2-58-95 was used at a fixed concentration and the unlabeled probe COX2-1-30 was present at increasing concentrations (Fig. 4D). Moreover, each probe appeared to outcompete the other one when added in excess, with the target in the 5'-UTR exhibiting a higher affinity to the protein. Thus, our data suggest that rPet111p can only bind to one RNA target at a time, and therefore, at least some of the RNA recognition and/or binding elements in the protein may be involved in interaction with each of the two targets.

Discussion

Genetic studies in yeast have identified a set of nuclear gene products that activate the translation of mitochondrial mRNAs (2–4). One of these factors, Pet111p, is specifically required for the translation of COX2 mRNA (6) and was suggested to act by a direct association with the 5'-UTR of the transcript (13). However, this suggestion has not yet been verified experimen-

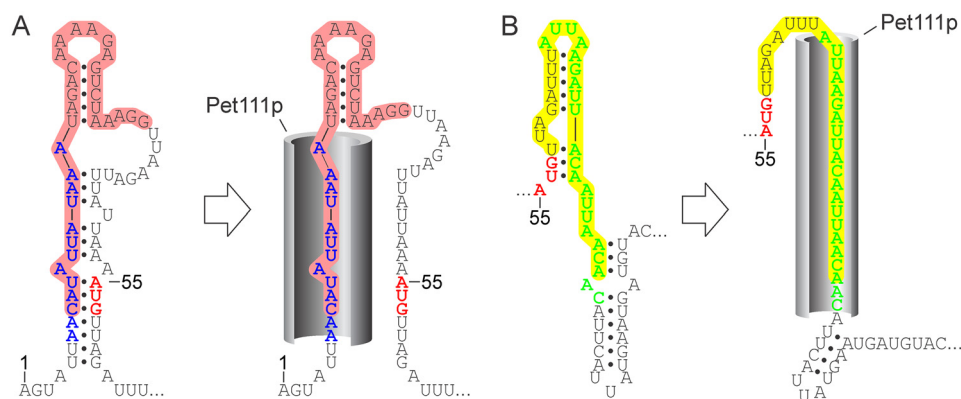


Figure 5. A possible mechanism of activation of COX2 translation by Pet11p. *A*, a structure formed by the 5'-UTR and a region in the beginning of the ORF as previously proposed (24) is shown on the left. The blue lettering indicates the UTR target of rPet11p. The region highlighted in pink contains residues required for respiration (19). *B*, a previously suggested alternative structure involving the beginning of the ORF is shown on the left (20). The Pet11p ORF target is shown in green lettering. Deletions or substitutions of certain nucleotides within the sequence highlighted in yellow, either in the WT or 70A>C;72A>U background, disrupted translation (20). On the right of both panels, it is shown how binding of Pet11p (gray hollow cylinders) to corresponding targets would prevent the RNA structures from forming, making the region of the start codon (red lettering) single-stranded and available for translation. *B*, binding of Pet11p at the ORF target is also expected to interfere with a downstream stem-loop structure. Destabilization of this structure was reported to promote translation of COX2 (20).

tally, nor has a mechanism been proposed by which the presumed interaction could lead to the activation of translation. Here, we set out to examine the relationship between Pet11p and COX2 in greater detail. We found that the protein is indeed associated predominantly with COX2 *in vivo* (Fig. 1) and binds directly to two distinct RNA targets *in vitro* (Fig. 3). We mapped the targets to the regions 7–19 (5'-UTR target) and 66–86 (ORF target) relative to the transcription start site (Fig. 4, *A* and *B*). Obviously, not all nucleotides within the mapped boundaries may be critical for the specific binding of Pet11p. The sequences that are actually recognized are expected to be somewhat shorter and may be discontinuous. A comprehensive mutagenesis analysis is needed to identify the RNA bases that constitute the actual signals recognized by the protein.

The two identified targets of Pet11p vary in length and do not contain an apparent common sequence pattern that would be stringent enough to set these regions apart from the rest of the mitochondrial RNA. It is not obvious how a single protein can recognize these two diverse targets. Our EMSA data show that the protein can only bind to one of the targets at a time (Fig. 4*D*), which could be either due to a steric overlap of the two RNA-binding sites or because some elements in the protein are engaged during the recognition of either target. Alternatively, Pet11p may undergo structural reorganization to adapt to certain targets, but not others, by an induced fit mechanism. In this scenario, the same structural elements may be involved in different modes of specific binding to each of the two targets depending on the RNA sequence context and the structural configuration of the corresponding RNA recognition modules in the protein.

It is currently unclear how binding of Pet11p may promote the translation of COX2. In general, the protein could modify the structure of the message, facilitate the recruitment of the ribosome at the site of initiation, or stabilize the association of the mRNA with other yet-unknown factors needed for efficient translation. A recent study has shown that the mitochondrial ribosome cannot associate with COX2 in Δ *pet111* cells, whereas binding to other mRNAs is not significantly affected

(23); however, the mechanism behind this effect is unclear. It has been predicted that the 5'-end proximal region in COX2 may assume the fold shown in Fig. 5*A* (24). In this structure, a sequence in the vicinity of the translation initiation codon is base-paired with the upstream RNA. Remarkably, most of the upstream sequence involved in the duplex overlaps with the Pet11p 5'-UTR target mapped in this study. Therefore, binding of Pet11p would prevent the duplex from forming, thus making the translation initiation region single-stranded and accessible to the ribosome. A comprehensive mutagenesis analysis of the COX2 5'-UTR has revealed a 31-nt region, located between positions 9 and 39, where substitutions led to a loss of translation of the mutant mRNA and cellular respiration (19). Significantly, the Pet11p 5'-UTR-binding target substantially overlaps with the upstream part of this region (Fig. 5*A*). Curiously, the reported mutants demonstrated two clearly distinct phenotypes. Substitutions downstream from position A23 did not significantly destabilize the mutant mRNAs, but inhibited their translation. Conversely, a drastic decrease in the mRNA levels was added to the translational defects when the nucleotides upstream from position C24 were mutated. These latter mutations alter the Pet11p 5'-UTR target and would be expected to interfere with the binding of the protein. Because inactivation of *pet111* was reported to cause up to a 10-fold decrease in levels of COX2 (6), the observed destabilization of the mutant mRNAs was likely caused by the loss of protection by Pet11p. The loss of translation resulting from the substitutions (19) and deletions (13) introduced into the 5'-UTR downstream from the Pet11p target suggests that a second enhancer of translation may be present there. This element may function at the RNA level or serve as a binding site for an additional translational activator. Taking all of the above considerations into account, our mapping of the Pet11p 5'-UTR-binding target is consistent with results of previous genetic, *in vivo* biochemistry, and structural prediction analysis of the 5'-leader.

The finding that Pet11p contacts COX2 inside the ORF was surprising, because none of the mRNA-specific yeast mitochondrial translational activators were previously reported to

act outside of the 5'-UTRs. Remarkably, the only known mammalian mitochondrial translational activator, TACO1, has recently been shown to bind selectively to the ORF of *COX1* (25). Our data thus indicate that a similar phenomenon may also exist in yeast, and regulation of yeast mitochondrial translation may involve binding of activators inside ORFs. Significantly, translation of a chimeric mRNA, in which the *COX2* ORF was fused to an upstream *COX3* 5'-UTR sequence, was possible in the absence of Pet111p (7). Therefore, if the binding of Pet111p to the ORF target is required for translation in the WT background, this requirement must be dictated by an element present in the *COX2* 5'-UTR and is bypassed when the entire leader is replaced. However, the functional significance of the binding of Pet111p at this site is yet to be confirmed genetically. Previous work has shown that a positively acting translation control element is embedded in the region that encodes the first 14 amino acids of the Cox2p precursor and that the sequence comprising codons 2–6 is critical for the function of this element (20). The sequence of codons 7–10 was also important for translation when codon 6 was mutated. Notably, the mapped Pet111p ORF target, which approximately corresponds to codons 5–11, partially overlaps with this control element (Fig. 5B). The reported translational and respiratory defects induced by mutations within the first 10 codons of *COX2* may therefore result from weakening the interaction between Pet111p and its ORF target. Consistently, these defects were relieved in cells overexpressing Pet111p (20), although an effect of the overexpression on the interaction of Pet111p with the 5'-UTR target might have also contributed to the suppression. The proximal region of the *COX2* ORF was suggested to fold into a structure (20) such that the nucleotides at the site of translation initiation are base-paired with a downstream sequence, which is included in the ORF-binding target of Pet111p (Fig. 5B). Therefore, similar to the mechanism suggested in Fig. 5A, binding of the protein would be expected to prevent the base pairing of the initiation region, making it available for association with the ribosome. The two putative structures shown in Fig. 5 do not appear to be compatible, and thus the mRNA may alternate between the two states. Simultaneous binding of two Pet111p molecules at both targets may be necessary to prevent base pairing of the translation initiation region. In addition, a translation-inhibiting element has been identified in the sequence comprising codons 15–25 (26), and a part of this sequence is predicted to form a stem-loop structure with an upstream region (20) as shown in Fig. 5B. Weakening the structure by deletion or substitution of the involved nucleotides diminished the translation-inhibiting effect of this element (20, 26). Importantly, the ORF target of Pet111p partially overlaps with the sequence of the upstream strand of the stem of the structure. Therefore, binding of the protein should interfere with the formation of the structure, thereby providing additional means to promote *COX2* translation. Although the proposed model of translational activation by Pet111p is certainly speculative, it is remarkable that a very similar mechanism has been shown to facilitate the translation of mRNA in maize chloroplasts. In this mechanism, binding of PPR10 in the 5'-UTR of *ATP-H* induces structural remodeling in the initia-

tion region, which liberates the Shine–Dalgarno sequence and thus enables translation (27).

Based on bioinformatic analysis, Pet111p has been assigned as a member of the pentatricopeptide repeat (PPR) protein family (28). Especially numerous in plant organelles (29), PPR proteins generally function in post-transcriptional RNA metabolism by associating with predominantly single-stranded RNA targets in a sequence-specific manner (30). Plant PPR proteins recognize their targets using domains composed of multiple 35-amino acid PPR motifs. The recognition occurs in a modular mode, at a ratio of one RNA base per one PPR motif, and in accordance with a set of principles known as the PPR code (31). Only three *Saccharomyces cerevisiae* proteins (Aep3p, Dmr1p, and Pet309p) were found to contain the sequence motifs that matched the plant PPR pattern (32). Although the general functional profile of a group of 12 additional PPR proteins identified in yeast (28) appears to be consistent with that of the plant PPR proteins, the sequence signature of their PPR motifs is evidently distinct (33). It is therefore not clear whether the yeast PPR proteins utilize the same mechanistic patterns as those in plants. Our data indicate that Pet111p, a protein from the yeast PPR subfamily, can interact with single-stranded RNA directly and sequence-specifically. However, it remains to be determined whether this recognition utilizes a PPR code similar to the one in plants and whether it is modular in nature. To better understand the function of yeast PPR proteins, more information on the corresponding protein–RNA interacting pairs is needed. Other gene-specific translational activators that are presumed to selectively interact with targets in the yeast mitochondrial mRNAs have been classified as PPR proteins (28). The approach presented in this work opens a way to mapping the targets of these proteins with high precision.

Experimental procedures

Oligonucleotides

Synthetic DNA oligonucleotides were purchased from Integrated DNA Technology, and synthetic RNA was from GE Healthcare Dharmacon and Integrated DNA Technology (sequences are listed in Table S1). The RNA probes used in the EMSA and RNase footprinting experiments were 5'-labeled and gel-purified as described in the supporting information.

PAR-CLIP analysis

PAR-CLIP and data acquisition were performed as described in the supporting information. Data quality control and mapping were performed as described (34). Briefly, sequencing reads were quality trimmed and mapped to the *S. cerevisiae* genome (sacCer3, version 64.2.1) using the short read aligner STAR version 2.5.2b (35). Coverage plots were generated using GenomicAlignments (36).

Determination of the mature N terminus of Pet111p

Mitochondria were isolated from yeast expressing tagged Pet111p as specified in the supporting information. Approximately 0.3 ml of settled mitochondria were resuspended in 1.2 ml of lysis solution (7 M guanidine HCl, 100 mM NaCl, 15 mM imidazole, 3 mM β -mercaptoethanol), and the suspension was

sonicated on ice with five 30-s pulses intermitted with 30-s pauses on a F60 sonic dismembrator (Fisher Scientific). The lysate was cleared by centrifugation ($20,000 \times g$, 15 min), and the supernatant was incubated with 20 μ l of Ni-IDA-agarose beads (Gold Biotechnology) in a tumbling tube overnight at room temperature. The beads were then washed three times with the lysis solution and two times with water using 1.4 ml/wash. The bound proteins were eluted with 80 μ l of 1 \times lithium dodecyl sulfate gel loading buffer (Novex, Life Technologies), a 20- μ l sample of the eluate was separated by 4–12% lithium dodecyl sulfate-PAGE, and the protein bands were visualized by Coomassie staining. The band that corresponded to the tagged Pet11p was identified by PMF as described in the [supporting information](#). The eluted proteins were separated by PAGE once again and transferred onto an Immobilon-PSQ membrane (EMD Millipore) by electroblotting, and the tagged Pet11p band was cut out from the membrane and submitted for N-terminal sequencing (Midwest Analytical).

Expression and purification of rPet11p

E. coli XJb(DE3) cells (Zymo Research) were transformed with plasmid pGD1, and rPet11p was expressed at a temperature of 12 °C. The protein was purified sequentially on a nickel-agarose column, by heparin-affinity chromatography, and gel filtration as described in the [supporting information](#).

Mapping of the 5'-end in mature COX2

DNA primer COX2-96-76 was hybridized to COX2 in a preparation of total mitochondrial RNA and extended with RT as detailed in the [supporting Experimental procedures](#).

Electrophoretic mobility shift assays

rPet11p was combined with 5'-³²P-labeled RNA probes (0.1 μ M) in 10 μ l of binding buffer (20 mM Tris-HCl, pH 7.2, 50 mM NaCl, 5 mM MgCl₂, 5% glycerol). Yeast tRNA (Sigma) was added at a 2-fold molar excess over the protein (or 1 μ M in [Fig. 4D](#)) to reduce nonspecific binding, and the mixtures were incubated for 20 min at 30 °C. The mixtures were supplemented with 2 μ l of 30% glycerol spiked with xylene cyanol and bromophenol blue and loaded on 8% (37.5:1, acrylamide:bisacrylamide) polyacrylamide gels cast in the presence of 1 \times Tris borate/EDTA buffer. Electrophoresis was performed at room temperature in 0.5 \times Tris borate/EDTA running buffer for 15 min at 175 V. Radioactive bands corresponding to protein-RNA complexes and unbound RNA were visualized using storage phosphor screens and a Typhoon 9410 scanner (GE Healthcare).

RNase footprinting

5'-³²P-labeled RNA probes were incubated with rPet11p (where indicated) in 10 μ l of binding buffer (specified above) for 20 min at 30 °C. Yeast tRNA (1 and 1.2 μ M in the experiments shown in [Fig. 4, A and B](#), respectively) was present in the mixtures. RNase I (New England Biolabs) was then added to a concentration of 8 units/ml where indicated, and the mixtures were incubated for 16 min at 30 °C. RNase A (Qiagen) was used at a concentration of 0.8 ng/ml where indicated. The reactions were stopped by mixing them with 10 μ l of gel loading buffer (50 mM

EDTA in 95% formamide spiked with xylene cyanol and bromophenol blue) and heating at 95 °C for 5 min. The products of digestion were separated in gradient thickness (0.4–1.2 mm) 20% (19:1, acrylamide:bisacrylamide) gels cast with 7 M urea. The radioactive RNA species were visualized by phosphor imaging with a Typhoon 9410 scanner (GE Healthcare) and quantified using ImageQuant 5.2 software (Molecular Dynamics).

Author contributions—J. L. J., P. C., and M. A. validation; J. L. J., K. B. H., A. T. C., D. T., and M. A. investigation; J. L. J. and K. B. H. visualization; J. L. J., K. B. H., D. T., P. C., and M. A. methodology; K. B. H., A. T. C., and M. A. data curation; K. B. H. formal analysis; K. B. H., D. T., P. C., and M. A. writing-original draft; D. T. and M. A. writing-review and editing; P. C. and M. A. conceptualization; P. C. and M. A. supervision; P. C. and M. A. funding acquisition.

Acknowledgments—We thank William McAllister for critically reading the manuscript and useful suggestions. We also thank Claire Corbett and Gary Devine for technical assistance during the initial stages of this project.

References

1. Strecker, V., Kadeer, Z., Heidler, J., Cruciati, C.-M., Angerer, H., Giese, H., Pfeiffer, K., Stuart, R. A., and Wittig, I. (2016) Supercomplex-associated Cox26 protein binds to cytochrome *c* oxidase. *Biochim. Biophys. Acta* **1863**, 1643–1652 [CrossRef Medline](#)
2. Ott, M., Amunts, A., and Brown, A. (2016) Organization and regulation of mitochondrial protein synthesis. *Annu. Rev. Biochem.* **85**, 77–101 [CrossRef Medline](#)
3. Herrmann, J. M., Woellhaf, M. W., and Bonnefoy, N. (2013) Control of protein synthesis in yeast mitochondria: the concept of translational activators. *Biochim. Biophys. Acta* **1833**, 286–294 [CrossRef Medline](#)
4. Fox, T. D. (2012) Mitochondrial protein synthesis, import, and assembly. *Genetics* **192**, 1203–1234 [CrossRef Medline](#)
5. Strick, C. A., and Fox, T. D. (1987) *Saccharomyces cerevisiae* positive regulatory gene PET111 encodes a mitochondrial protein that is translated from an mRNA with a long 5' leader. *Mol. Cell Biol.* **7**, 2728–2734 [CrossRef Medline](#)
6. Poutre, C. G., and Fox, T. D. (1987) PET111, a *Saccharomyces cerevisiae* nuclear gene required for translation of the mitochondrial mRNA encoding cytochrome *c* oxidase subunit II. *Genetics* **115**, 637–647 [Medline](#)
7. Mulero, J. J., and Fox, T. D. (1993) Pet111 Acts in the 5'-leader of the *Saccharomyces cerevisiae* mitochondrial Cox2 mRNA to promote its translation. *Genetics* **133**, 509–516 [Medline](#)
8. Green-Willms, N. S., Butler, C. A., Dunstan, H. M., and Fox, T. D. (2001) Pet11p, an inner membrane-bound translational activator that limits expression of the *Saccharomyces cerevisiae* mitochondrial gene COX2. *J. Biol. Chem.* **276**, 6392–6397 [CrossRef Medline](#)
9. Sanchirico, M. E., Fox, T. D., and Mason, T. L. (1998) Accumulation of mitochondrially synthesized *Saccharomyces cerevisiae* Cox2p and Cox3p depends on targeting information in untranslated portions of their mRNAs. *EMBO J.* **17**, 5796–5804 [CrossRef Medline](#)
10. Naithani, S., Saracco, S. A., Butler, C. A., and Fox, T. D. (2003) Interactions among COX1, COX2, and COX3 mRNA-specific translational activator proteins on the inner surface of the mitochondrial inner membrane of *Saccharomyces cerevisiae*. *Mol. Biol. Cell* **14**, 324–333 [CrossRef Medline](#)
11. Krause, K., Lopes de Souza, R., Roberts, D. G., and Dieckmann, C. L. (2004) The mitochondrial message-specific mRNA protectors Cbp1 and Pet309 are associated in a high-molecular weight complex. *Mol. Biol. Cell* **15**, 2674–2683 [CrossRef Medline](#)
12. Kehrein, K., Schilling, R., Möller-Hergt, B. V., Wurm, C. A., Jakobs, S., Lamkemeyer, T., Langer, T., and Ott, M. (2015) Organization of mito-

- chondrial gene expression in two distinct ribosome-containing assemblies. *Cell Reports* **10**, 843–853 [CrossRef Medline](#)
13. Mulero, J. J., and Fox, T. D. (1993) Alteration of the *Saccharomyces cerevisiae* COX2 mRNA 5'-untranslated leader by mitochondrial gene replacement and functional interaction with the translational activator protein PET111. *Mol. Biol. Cell* **4**, 1327–1335 [CrossRef Medline](#)
14. Gelperin, D. M., White, M. A., Wilkinson, M. L., Kon, Y., Kung, L. A., Wise, K. J., Lopez-Hoyo, N., Jiang, L., Piccirillo, S., Yu, H., Gerstein, M., Dumont, M. E., Phizicky, E. M., Snyder, M., and Grayhack, E. J. (2005) Biochemical and genetic analysis of the yeast proteome with a movable ORF collection. *Genes Dev.* **19**, 2816–2826 [CrossRef Medline](#)
15. Henzel, W. J., Watanabe, C., and Stults, J. T. (2003) Protein identification: the origins of peptide mass fingerprinting. *J. Am. Soc. Mass Spectrom.* **14**, 931–942 [CrossRef Medline](#)
16. Wiesenberger, G., and Fox, T. D. (1997) Pet127p, a membrane-associated protein involved in stability and processing of *Saccharomyces cerevisiae* mitochondrial RNAs. *Mol. Cell Biol.* **17**, 2816–2824 [CrossRef Medline](#)
17. Coruzzi, G., Bonitz, S. G., Thalenfeld, B. E., and Tzagoloff, A. (1981) Assembly of the mitochondrial membrane system: analysis of the nucleotide sequence and transcripts in the oxl1 region of yeast mitochondrial DNA. *J. Biol. Chem.* **256**, 12780–12787 [Medline](#)
18. Costanzo, M. C., Bonnefoy, N., Williams, E. H., Clark-Walker, G. D., and Fox, T. D. (2000) Highly diverged homologs of *Saccharomyces cerevisiae* mitochondrial mRNA-specific translational activators have orthologous functions in other budding yeasts. *Genetics* **154**, 999–1012 [Medline](#)
19. Dunstan, H. M., Green-Willms, N. S., and Fox, T. D. (1997) *In vivo* analysis of *Saccharomyces cerevisiae* COX2 mRNA 5'-untranslated leader functions in mitochondrial translation initiation and translational activation. *Genetics* **147**, 87–100 [Medline](#)
20. Bonnefoy, N., Bsat, N., and Fox, T. D. (2001) Mitochondrial translation of *Saccharomyces cerevisiae* COX2 mRNA is controlled by the nucleotide sequence specifying the pre-Cox2p leader peptide. *Mol. Cell Biol.* **21**, 2359–2372 [CrossRef Medline](#)
21. Nilsen, T. W. (2014) RNase footprinting to map sites of RNA–protein interactions. *Cold Spring Harbor Protocols* **2014**, 677–682 [Medline](#)
22. Meador, J., 3rd, Cannon, B., Cannistraro, V. J., and Kennell, D. (1990) Purification and characterization of *Escherichia coli* RNase I. *Eur. J. Biochem.* **187**, 549–553 [CrossRef Medline](#)
23. Couvillion, M. T., Soto, I. C., Shipkovenska, G., and Churchman, L. S. (2016) Synchronized mitochondrial and cytosolic translation programs. *Nature* **533**, 499–503 [CrossRef Medline](#)
24. Papadopoulou, B., Dekker, P., Blom, J., and Grivell, L. A. (1990) A 40 kd protein binds specifically to the 5'-untranslated regions of yeast mitochondrial mRNAs. *EMBO J.* **9**, 4135–4143 [CrossRef Medline](#)
25. Richman, T. R., Spähr, H., Ermer, J. A., Davies, S. M., Viola, H. M., Bates, K. A., Papadimitriou, J., Hool, L. C., Rodger, J., Larsson, N.-G., Rackham, O., and Filipovska, A. (2016) Loss of the RNA-binding protein TACO1 causes late-onset mitochondrial dysfunction in mice. *Nat. Commun.* **7**, 11884 [CrossRef Medline](#)
26. Williams, E. H., and Fox, T. D. (2003) Antagonistic signals within the COX2 mRNA coding sequence control its translation in *Saccharomyces cerevisiae* mitochondria. *RNA* **9**, 419–431 [CrossRef Medline](#)
27. Prikryl, J., Rojas, M., Schuster, G., and Barkan, A. (2011) Mechanism of RNA stabilization and translational activation by a pentatricopeptide repeat protein. *Proc. Natl. Acad. Sci. U.S.A.* **108**, 415–420 [CrossRef Medline](#)
28. Lipinski, K. A., Puchta, O., Surendranath, V., Kudla, M., and Golik, P. (2011) Revisiting the yeast PPR proteins: application of an iterative hidden Markov model algorithm reveals new members of the rapidly evolving family. *Mol. Biol. Evol.* **28**, 2935–2948 [CrossRef Medline](#)
29. Schmitz-Linneweber, C., and Small, I. (2008) Pentatricopeptide repeat proteins: a socket set for organelle gene expression. *Trends Plant Sci.* **13**, 663–670 [CrossRef Medline](#)
30. Barkan, A., and Small, I. (2014) Pentatricopeptide repeat proteins in plants. *Annu. Rev. Plant Biol.* **65**, 415–442 [CrossRef Medline](#)
31. Barkan, A., Rojas, M., Fujii, S., Yap, A., Chong, Y. S., Bond, C. S., and Small, I. (2012) A combinatorial amino acid code for RNA recognition by pentatricopeptide repeat proteins. *PLoS Genet.* **8**, e1002910 [CrossRef Medline](#)
32. Small, I. D., and Peeters, N. (2000) The PPR motif: a TPR-related motif prevalent in plant organellar proteins. *Trends Biochem. Sci.* **25**, 46–47 [Medline](#)
33. Herbert, C. J., Golik, P., and Bonnefoy, N. (2013) Yeast PPR proteins, watchdogs of mitochondrial gene expression. *RNA Biol.* **10**, 1477–1494 [CrossRef Medline](#)
34. Baejen, C., Torkler, P., Gressel, S., Essig, K., Söding, J., and Cramer, P. (2014) Transcriptome maps of mRNP biogenesis factors define pre-mRNA recognition. *Mol. Cell* **55**, 745–757 [CrossRef Medline](#)
35. Dobin, A., Davis, C. A., Schlesinger, F., Drenkow, J., Zaleski, C., Jha, S., Batut, P., Chaisson, M., and Gingeras, T. R. (2013) STAR: ultrafast universal RNA-seq aligner. *Bioinformatics* **29**, 15–21 [CrossRef Medline](#)
36. Lawrence, M., Huber, W., Pagès, H., Aboyoun, P., Carlson, M., Gentleman, R., Morgan, M. T., and Carey, V. J. (2013) Software for computing and annotating genomic ranges. *PLoS Comput. Biol.* **9**, e1003118 [CrossRef Medline](#)
37. Fukasawa, Y., Tsuji, J., Fu, S.-C., Tomii, K., Horton, P., and Imai, K. (2015) MitoFates: improved prediction of mitochondrial targeting sequences and their cleavage sites. *Mol. Cell. Proteomics* **14**, 1113–1126 [CrossRef Medline](#)
38. Osinga, K. A., De Vries, E., Van der Horst, G., and Tabak, H. F. (1984) Processing of yeast mitochondrial messenger RNAs at a conserved decamer sequence. *EMBO J.* **3**, 829–834 [CrossRef Medline](#)

Yeast mitochondrial protein Pet111p binds directly to two distinct targets in *COX2* mRNA, suggesting a mechanism of translational activation

Julia L. Jones, Katharina B. Hofmann, Andrew T. Cowan, Dmitry Temiakov, Patrick Cramer and Michael Anikin

J. Biol. Chem. 2019, 294:7528-7536.

doi: 10.1074/jbc.RA118.005355 originally published online March 25, 2019

Access the most updated version of this article at doi: [10.1074/jbc.RA118.005355](https://doi.org/10.1074/jbc.RA118.005355)

Alerts:

- [When this article is cited](#)
- [When a correction for this article is posted](#)

[Click here](#) to choose from all of JBC's e-mail alerts

This article cites 38 references, 18 of which can be accessed free at <http://www.jbc.org/content/294/18/7528.full.html#ref-list-1>